

# Spectral Markers in Preneoplastic Intestinal Mucosa: An Accurate Predictor of Tumor Risk in the MIN Mouse

Hemant K. Roy,<sup>1</sup> Young L. Kim,<sup>2</sup> Ramesh K. Wali,<sup>1</sup> Yang Liu,<sup>2</sup> Jennifer Koetsier,<sup>1</sup> Dhananjay P. Kunte,<sup>1</sup> Michael J. Goldberg,<sup>1</sup> and Vadim Backman<sup>2</sup>

<sup>1</sup>Department of Internal Medicine, Evanston-Northwestern Healthcare; <sup>2</sup>Biomedical Engineering Department, Northwestern University, Evanston, Illinois

## Abstract

**Background:** We have reported recently that microarchitectural analysis of the histologically normal mucosa using a novel optics technology, four-dimensional elastic light scattering fingerprinting (ELF), provided unprecedented sensitivity for early detection of colon carcinogenesis. In the present study, we explored the ability of four-dimensional ELF to identify an inherited predisposition to colorectal cancer, an issue of considerable importance for optimizing population screening strategies.

**Methods:** We used the MIN mouse, a model whose germ line adenomatous polyposis coli truncation leads to spontaneous intestinal tumorigenesis, thus replicating the human syndrome, familial adenomatous polyposis. Spectral markers were assessed by four-dimensional ELF analysis in MIN mice at preneoplastic time points and compared with age-matched controls (C57BL/6 mice with wild-type adenomatous polyposis coli). To assess the responsiveness of spectral markers to chemopreventive agents, a subset of MIN mice was supplemented with celecoxib 1,500 ppm.

**Results:** Spectral slope, fractal dimension, and principal component 3 were dramatically altered in the uninvolved MIN mouse mucosa at the earliest time points. Furthermore, alteration in spectral variables increased over time, consonant with the microarchitectural underpinnings of subsequent tumorigenesis. Additionally, these markers spatially correlated with future adenoma development (small intestine > colon). Short-term treatment with the potent chemopreventive agent, celecoxib, resulted in near normalization of fractal dimension and principal component 3.

**Conclusions:** We report, for the first time, that spectral markers, assayed by four-dimensional ELF, were able to sensitively identify a genetic predisposition for intestinal tumorigenesis before the occurrence of phenotypic manifestations. Moreover, the reversal of spectral markers by celecoxib treatment supports the neoplastic relevance. (Cancer Epidemiol Biomarkers Prev 2005; 14(7):1639–45)

## Introduction

Colorectal cancer remains the second leading cause of cancer death in the United States, estimated to result in 56,290 fatalities in 2005 (1). Colorectal cancer deaths are eminently preventable through colonoscopic screening (2). However, due to resource availability, cost, patient reluctance, and potential complications, only a small fraction of the population undergoes the “gold standard” procedure for colon cancer prevention. Targeting patients at increased risk of colorectal cancer for colonoscopy is crucial for maximizing benefits and minimizing risk/costs. An inherited predilection is one of the most important risk factors, implicated in 20% to 30% of all colorectal cancers (3). This familial predisposition to colorectal cancer encompasses a wide spectrum of phenotypic consequences ranging from low-penetrance polymorphisms, which engender a 1.5- to 3-fold increased risk [e.g., adenomatous polyposis coli (APC) I1307K], to autosomal dominant syndromes that place patients at extraordinarily high risk for colorectal cancer, such as familial adenomatous polyposis (FAP) or hereditary nonpolyposis colorectal cancer (3).

Although there has been considerable progress in understanding the genetic susceptibility to colorectal cancer, the

current clinical state-of-the-art is suboptimal. Although patients are accurate regarding their family history (4), determination of the members of the kindred who have actually acquired the colorectal cancer risk remains challenging because of the unclear genetic basis for the vast majority of cases. Moreover, even when genetic testing is available, the phenotypic heterogeneity complicates the choice of optimal colorectal cancer prevention strategies (5).

Analyzing the colonic mucosa is a powerful means of ascertaining the colorectal cancer risk. Indeed, by exploiting the “field effect” of colon carcinogenesis, one can potentially obtain a global overview of future neoplastic risk by evaluating the distal colon. Several lines of evidence suggest that analyzing the uninvolved colonic epithelium may allow estimation of risk before occurrence of phenotype (adenomas or carcinomas). For instance, colonocyte proliferation rate is markedly augmented in nonneoplastic rectal mucosa from both FAP patients and sporadic patients who harbor adenomas (6, 7). Apoptosis assays in the distal colon have also been shown to predict concurrent colonic neoplasia (8). In the histologically normal intestinal mucosa of the MIN (multiple intestinal neoplasia) mouse (the murine equivalent of FAP), there is dramatic up-regulation of several proto-oncogenes that preceded macroscopic neoplasia development (9). However, assaying these cellular and genetic markers is imprecise and cumbersome and therefore impractical for clinical utilization. Cellular microarchitecture may represent an exquisitely sensitive modality to reflect the genetic/environmental milieu during early carcinogenesis; however, the methodological barriers have stymied utilization for screening (10).

We, in collaboration with others, have pioneered the use of light scattering spectroscopy to noninvasively analyze nuclear size and chromatin texture to diagnose dysplasia in general

Received 11/13/04; revised 2/26/05; accepted 5/2/05.

**Grant support:** NIH (National Cancer Institute grants 1R21CA102750-01 and 1R03CA10549-01 and Early Detection Research Network grant 1U01CA11125-01), National Science Foundation grant BES-0238903, and American Cancer Society-Illinois Division.

The costs of publication of this article were defrayed in part by the payment of page charges. This article must therefore be hereby marked advertisement in accordance with 18 U.S.C. Section 1734 solely to indicate this fact.

**Requests for reprints:** Hemant K. Roy, Feinberg School of Medicine at Northwestern University, Department of Internal Medicine, Evanston Northwestern Healthcare, 2650 Ridge Avenue, Evanston, IL 60201. Phone: 847-570-2339; Fax: 847-657-1961. E-mail: h-roy@northwestern.edu

Copyright © 2005 American Association for Cancer Research.

and specifically in the colon (11, 12). However, this first generation technology was unable to harness the full spectrum of information regarding the size, shape, internal organization of cell microarchitecture, and relationship to surrounding intracellular milieu that are encoded in light scattering signals. To overcome these limitations, we developed four-dimensional elastic light scattering fingerprinting (ELF), which assesses a wide spectrum of light scattering variables, including wavelength of light, scattering angle, azimuthal angle, and polarization of scattered light (13). Four-dimensional ELF is a novel light scattering technology that gives unprecedented quantitative information about tissue structures ranging in size from tens of nanometers to micron range (i.e., macromolecular complexes to organelles). We have shown recently that microarchitectural alterations ascertained by four-dimensional ELF had remarkable sensitivity for the earliest events (before aberrant crypt foci formation) in colon carcinogenesis using the azoxymethane-treated rat model (14). In the present study, we used four-dimensional ELF to assess spectral markers in the preneoplastic MIN mouse mucosa as a means of identifying a genetic predisposition for intestinal tumorigenesis (i.e., mutation in the *APC* gene). We confirm carcinogenic relevance of these spectral markers by demonstrating both temporal and spatial correlations with future neoplasia as well as reversal with the potent chemopreventive agent celecoxib.

## Materials and Methods

**Animals.** All animal studies were done in accordance with the Institutional Animal Care and Use Committee of Evanston-Northwestern Healthcare (Evanston, IL). Twenty male MIN mice and 20 controls (C57BL6) mice were obtained (The Jackson Laboratory, Bar Harbor, ME) at ages 5 to 6 weeks. Animals were randomized to either AIN 76a diet alone (Teklad Labs, Indianapolis, IN) or the one supplemented with celecoxib 1,500 ppm. After being euthanized, the small intestine and colon were removed, longitudinally opened, washed with PBS, and examined under magnification for tumors.

**Four-Dimensional ELF Analysis.** We reported previously the development of four-dimensional ELF instrument to measure the most comprehensive light scattering data from living tissues recorded to date (13-15). Briefly, in this instrument, a series of points on a sample surface are illuminated by a collimated linearly polarized broadband light from a Xe-lamp. Tissue structures, ranging in size from nanometers to tens of microns, scatter the incident light. A portion of the scattered light escapes the tissue and is collected by the instrument. A Fourier lens positioned in the collection arm of the instrument projects the angular distribution of the light backscattered from the tissue onto the slit of a spectrometer, which further diverts this light now in the direction perpendicular to the slit depending on its spectral composition. The resulting two-dimensional image, wavelength  $\lambda$  (400-700 nm) versus scattering angle  $\theta$  ( $-7^\circ$  to  $7^\circ$ ), is projected onto a charge coupled device (Roper Scientific, Trenton, NJ) for a given azimuth of scattering  $\varphi$ , which can be varied by rotating a polarizer in the delivery arm of the system. The instrument also measures two independent polarization components  $p$  of the scattered light: one polarized along,  $I_{\parallel}$ , and orthogonally,  $I_{\perp}$ , to the incident polarization. Such four-dimensional data ( $\lambda, \theta, \varphi, p$ ) provide comprehensive information about the light scattering and can serve as extremely sensitive "fingerprints" of the specimen microarchitecture. Furthermore, the differential polarization signal  $\Delta I(\lambda) = I_{\parallel}(\lambda) - I_{\perp}(\lambda)$  is particularly sensitive to the superficial tissue ( $<50 \mu\text{m}$ ; e.g., mucosa). Signals  $I_{\parallel}, I_{\parallel} + I_{\perp}$ , and  $I_{\perp}$  contain information about progressively deeper tissues.

As discussed above, in each four-dimensional ELF measurement, we obtained light scattering data from  $\sim 2 \text{ mm}^2$  mouse intestinal mucosa. From each tissue site, three readings

were taken to ensure the consistency of the data. For each animal, four-dimensional ELF data were recorded from  $>20$  different tissue sites that were predetermined to uniformly span the surface of the distal small bowel and colon. The operators performing the four-dimensional ELF analysis were unaware of the genotype of the mouse. We predetermined the spectral markers to be assessed based on our previous studies.

**Spectral Markers.** To quantitate the microarchitecture, we assayed a variety of previously validated variables: spectral slope, fractal dimension, and principal components obtained via principal component analysis (PCA). These variables span the microarchitectural spectrum and thus are complementary in the characterization of nanoscale organization of the epithelium.

To characterize the spectral variations of  $\Delta I(\lambda)$ , we obtained linear fits to  $\Delta I(\lambda)$  using logistic regression. We showed that the absolute value of the linear coefficient of the fit, which is called the "spectral slope," may serve as an easily measurable marker to characterize the size distribution of structures within cells (14). This marker is particularly sensitive to the tissue structures ranging in size between 40 and 800 nm, which reflects tissue architecture from the size of macromolecular complexes to organelles (14).

Tissue organization at scales exceeding  $\sim 1 \mu\text{m}$  can be assessed by another marker that can be obtained from light scattering data, the fractal dimension (13, 16). Fractal dimension can be estimated from the angular distribution of the scattered light  $\Delta I(\theta, \lambda = \text{constant})$  for a wavelength fixed at the center of our wavelength range ( $\lambda = 550 \text{ nm}$ ; although the choice of the wavelength is not critical, the exact range of sizes for which the fractal properties are estimated may vary depending on the wavelength).  $\Delta I(\theta)$  was Fourier transformed to yield the two-point mass density correlation function  $C(r) = \langle \rho(r)\rho(r' + r) \rangle$ , where  $\rho(r)$  is a local mass density at point  $r$  (13, 14, 16). We found that for all tissue sites,  $C(r)$  followed a power law dependence on  $r$  for  $1 \mu\text{m} < r < 50 \mu\text{m}$ ,  $C(r) \propto r^{D-3}$ , where  $D$  is conventionally called fractal dimension. Thus, we obtained  $D$  from the linear slopes of  $C(r)$  in the linear regions of log-log scale.

Because of the complexity of light scattering data, not all features of ELF can be associated with specific physical properties of tissue. To gain further insights into the properties of ELF data, we also used PCA as one of the tools for characterizing light scattering data. PCA is a standard data reduction procedure for assessing underlying structure in a data set. In PCA, the light scattering spectra were averaged over scattering angles from  $-5^\circ$  to  $5^\circ$ . Each spectrum was preprocessed by mean scaling. A data matrix was created where each row of the matrix contained the preprocessed spectrum measurement and each column contained the preprocessed scattering intensity at each wavelength. The scores of all principal components were calculated using Matlab statistics toolbox software version 6.5 (The Mathworks, Inc., Natick, MA). Before investigating principal components as spectral markers of neoplasia, we first determined which principal components were of interest. Typically, in PCA, the first few principal components are responsible for most of the signal variation and the significance of higher-order principal components is minimal. We found that, in our data, principal components 1 to 3 accounted for  $\sim 99\%$  of the data variance, which justifies the use of these principal components to characterize the light scattering fingerprint data.

## Results

We investigated the ability of light scattering signatures obtained from four-dimensional ELF data to detect a genetic predisposition to intestinal tumorigenesis by using the MIN mouse model. The MIN mouse is a well-validated model that

spontaneously develops intestinal adenomas as a consequence of a germ line mutation in the *APC* tumor suppressor gene. We compared the light scattering signatures obtained from the MIN mice with age-matched C57BL mice that differed only in that they were wild-type (WT) at the *APC* locus. In the MIN mouse, >90% of intestinal adenomas occur in the small bowel and tumors occur in a well-established chronology, with no tumors noted in our study that exclusively focused on these early time points.

**Light Scattering Fingerprints.** Four-dimensional ELF data obtained from each point on a tissue surface have four dimensions of wavelength ( $\lambda$ ), scattering angle ( $\theta$ ), azimuth of scattering ( $\phi$ ), and polarization of scattered light. The light scattering "fingerprints" provide the most comprehensive representation of the information from light scattering, reflecting the size, structure, and associated milieu of the scattering objects. Given the large amount of data encompassed by these "fingerprints," this provides an extraordinarily sensitive albeit qualitative means of detecting alterations in microarchitectural changes in tissue architecture.

Figure 1 shows representative light scattering fingerprints from intestinal epithelium recorded from a MIN mouse at a preadenomatous stage (5-6 weeks old) and an age-matched control C57BL6 mouse. The light scattering fingerprints obtained from the distal small bowels of MIN and control mice revealed dramatic qualitative differences as indicated by changes in backscatter intensity (different colors) in the small intestine but not the colon. This finding accurately reflects the future occurrence of neoplasia in this model in that >90% of adenomas are located in the small bowel with minimal tumorigenesis in the colon (17, 18). Indeed, these data suggest that light scattering abnormalities predict a genetic substrate to neoplastic transformation before occurrence of neoplasia.

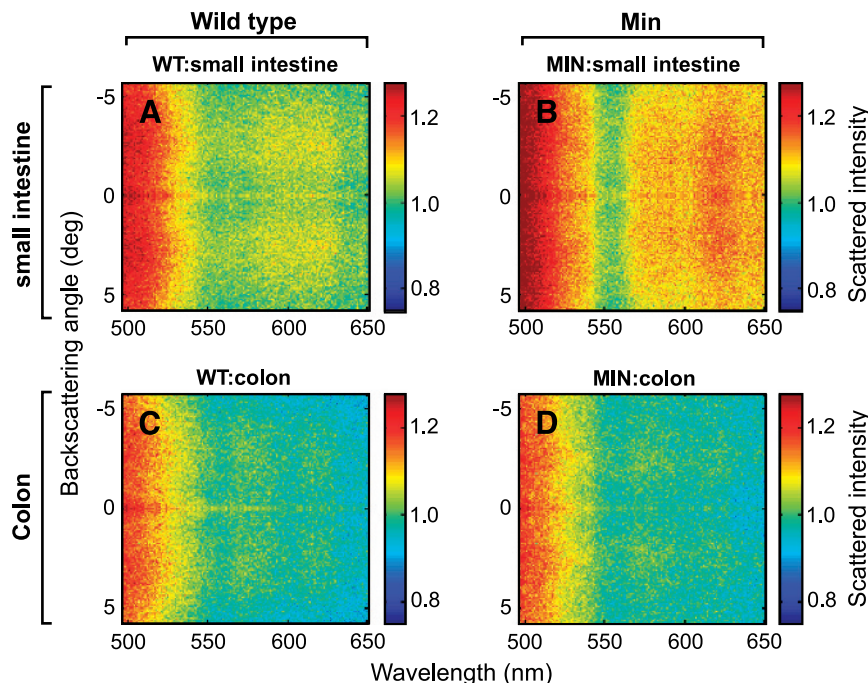
We identified several light scattering markers statistically highly significant for early neoplastic changes in MIN mice

and follow the temporal progression of intestinal tumorigenesis. We focused on the analysis of the light scattering fingerprint data in two dimensions: wavelength and scattering angle. To quantitate the light scattering and microarchitectural changes, we evaluated spectral markers that we discovered previously in the azoxymethane-treated rat model of experimental colorectal cancer. Specifically, we assayed three spectral markers: spectral slope (evaluating sizes from macromolecules to organelles), fractal dimension (measuring large organelles to groups of cells), and principal component 3. These variables are complimentary in characterization of tissue microarchitectural changes.

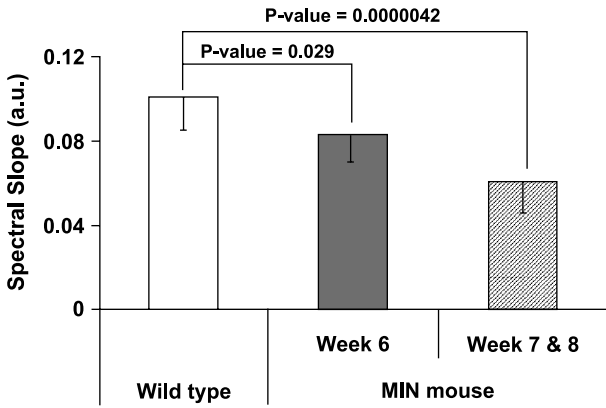
**Spectral Slope.** As discussed in Materials and Methods, the spectral slope is a variable that evaluates size distribution of particles ranging from macromolecules to organelles. Spectral behavior of differential polarization signal  $\Delta I(\lambda)$  depends on the size distribution of scattering structures. Generally,  $\Delta I(\lambda)$  is a declining function of wavelength and its steepness is related to the relative portion of structures of different sizes. Spectral slope is defined as the linear coefficient of the linear fit to  $\Delta I(\lambda)$ . Typically, larger structures ( $\sim 1 \mu\text{m}$ ) tend to reduce the steepness of the decline of  $\Delta I(\lambda)$  (i.e., small spectral slope), whereas smaller scatters with sizes much smaller than  $1 \mu\text{m}$  tend to make  $\Delta I(\lambda)$  decrease with wavelength steeper (i.e., large spectral slope; ref. 14).

Figure 2 shows the change of the spectral slope in the intestinal mucosa of 6-, 7-, and 8-week-old MIN and age-matched control mice. The spectral slope is dramatically decreased as early as in 6-week-old MIN mice compared with the controls ( $P < 0.05$ ) and continued to decrease at later time points (ANOVA  $P = 0.00004$ ). The progressive change in the spectral slope is consonant with the microarchitectural underpinnings of subsequent tumorigenesis.

We point out that our spectral data have been recorded at time points (i.e., 6- to 8-week-old mice) before the development



**Figure 1.** Representative four-dimensional ELF fingerprints from MIN or WT C57BL6 mice WT at the *APC* locus at a preneoplastic (6-week-old) time point. The color represents intensity of backscattering light. *X* axis, wavelength of the backscattering light; *Y* axis, backscattering angle. As shown, before the occurrence of tumors, the distal small bowel of the MIN mice had dramatically different light scattering fingerprints compared with WT animals. However, in the colon, where future neoplasia is minimal in this model, the MIN and WT "fingerprints" were quite similar.



**Figure 2.** Analysis of spectral information in the light scattering fingerprints. Spectral slope was obtained from the small intestine of MIN mice at preneoplastic time points. There was a progressive decrease in spectral slope consonant with increasing neoplastic transformation of the uninvolved mucosa that precedes frank adenoma formation.

of adenomas to avoid confounding effects of inadvertently assessing dysplastic tissue. As shown previously by several groups, in MIN mice, adenomas do not develop until much later, approximately at ages 10 to 12 weeks. This finding was also confirmed in our studies. Indeed, at ages 7 to 8 weeks, inspection of the intestine under magnification failed to show polyps. Thus, spectral slope may allow detection of carcinogenesis at a stage before the development of adenomas.

**Fractal Dimension.** We observed that fractal dimension was also markedly altered in the uninvolved intestinal mucosa of MIN mice as young as 6 weeks of age. Other groups have shown previously that fractal dimension may be used to detect esophageal carcinogenesis at a dysplastic stage (16). More recently, our group showed the potential of this variable to identify predysplastic stages of colorectal cancer in the azoxymethane-treated rat model (14). In both reports, the fractal dimension of neoplastic tissue was increased compared with its control values, thus indicating profound alteration of supramicron architecture of neoplastic mucosa (i.e., large organelle to groups of cells). As discussed in Materials and Methods, the angular distributions of the scattered light  $\Delta I(\theta)$  were used to calculate the fractal dimensions of tissue microarchitecture. As shown in Fig. 3, fractal dimension was elevated as early as in 6-week-old MIN mice ( $P < 0.001$ ) and continued to increase over time (ANOVA  $P < 0.001$ ). We point out that this change in fractal dimension was observed at a time point before the development of adenomas or other conventional biomarkers of colorectal cancer.

**Principal Component Analysis.** PCA is a standard variable reduction procedure that is commonly employed in biomedical research, including studies related to colorectal cancer biology (19, 20). The PCA of  $\Delta I(\lambda)$  revealed further changes in the light scattering signatures of MIN mice compared with those of age-matched WT mice. As shown in Fig. 4, the principal component 3 was increased in 6-week-old MIN mice and continued to progressively increase for the later time points, thus also following the progression of intestinal neoplasia ( $P < 10^{-14}$ ).

**Diagnostic Ability of Markers.** For light scattering markers to be clinically useful, not only do they have to detect early events in neoplasia, but also they have to enable identification of the at-risk group with high positive predictive value and negative predictive value. To determine the performance characteristics of an individual four-dimensional ELF measurement, we calculated the sensitivity, specificity, positive predic-

tive value, and negative predictive value for each individual point in the small intestine using the three spectral markers. As shown in Table 1, all variables exceeded 90% even for the earliest time points. Moreover, as expected, the accuracy of the light scattering diagnosis further increases with the progression of carcinogenesis. Such high positive predictive value and negative predictive value could not be achieved with any other currently used markers of colorectal cancer. Importantly, ELF enables highly accurate diagnosis of a genetic predisposition to tumorigenesis before the occurrence of the phenotype.

**Chemoprevention with Celecoxib.** To further validate the neoplastic relevance of the spectral markers in the uninvolved mucosa, we tested whether short-term treatment (1 week) of a chemopreventive agent, cyclooxygenase-2-specific non-steroidal anti-inflammatory drug celecoxib, would normalize the spectral markers in the preneoplastic MIN mouse mucosa. We chose celecoxib for this study because this agent has received regulatory approval for use in patients with FAP (the human equivalent of the MIN mouse). The dosage (1,500 ppm) was selected based on prior reports that this was not only well tolerated but also almost completely suppressed adenoma formation (21).

The normalization of spectral markers due to the effect of celecoxib is shown in Fig. 5. Remarkably, principal component 3 obtained from celecoxib-treated animals almost approached one measured from the WT mice. Moreover, in the celecoxib-treated mice, the fractal dimension was also markedly decreased, thereby approaching its control values. Spectral slope was the least responsive microarchitectural variable to celecoxib, failing to achieve statistical significance.

**Discussion**

We report herein, for the first time, dramatic microarchitectural alterations in the preneoplastic MIN mouse mucosa that preceded development of the phenotype (i.e., adenomas). Furthermore, these changes normalized with short-term treatment of the potent chemopreventive agent celecoxib. Thus, nanoscale structural analysis of the colonocyte represents a powerful means of detecting an inherited colorectal cancer risk and monitoring efficacy of chemopreventive agents. These observations were made possible because of the unprecedented sensitivity of four-dimensional ELF for assessing alterations in tissue microarchitecture.

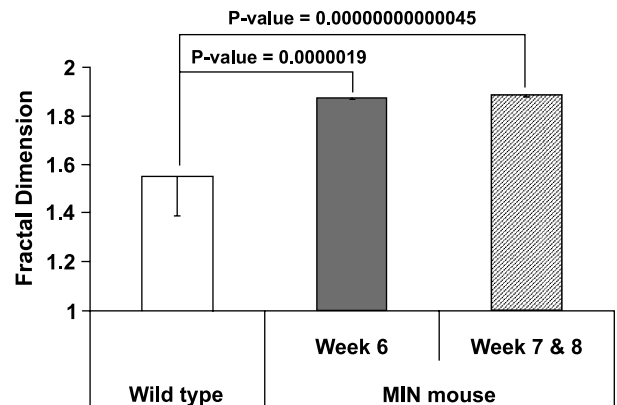


**Figure 3.** Analysis of scattering angle-dependent information in the light scattering fingerprints by quantitation of the fractal dimension of the superficial mucosa. Fractal dimension is significantly augmented in the initial stages of carcinogenesis (i.e., 6-week-old mice) and continued to increase at later preneoplastic time points, thus foreshadowing future intestinal neoplasia.

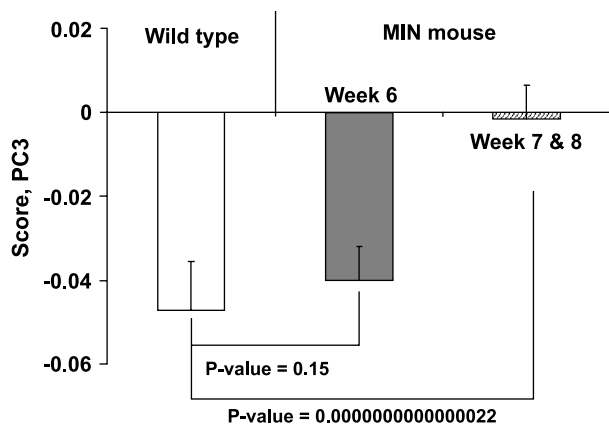


**Figure 4.** Principal component 3 was also significantly elevated in 6-week-old MIN mice and to progressively increase at the later preneoplastic time points in a manner consistent with future neoplastic transformation.

Four-dimensional ELF is a remarkable technological advance in that it can provide quantitative and highly reproducible data regarding structures that are 10 to 20 times smaller than detectable with conventional light microscopy.

Although the utilization of tissue microarchitecture to detect an inherited predisposition to colon carcinogenesis is novel, there are numerous lines of evidence to support its biological plausibility. Here, we review some of the previous findings that support the field effect in the MIN mouse, human familial colon cancer, and sporadic colon carcinogenesis. In the MIN mouse, there is unequivocal evidence that there are marked biochemical and genetic molecular abnormalities even in the histologically normal intestinal mucosa of the MIN mouse. For instance, when the preneoplastic intestinal mucosa of the MIN mouse was compared with age-matched WT mice, there are profound alterations in expression of genes, such as *cyclooxygenase-2*, *CXC cytokine receptor 2*, *interleukin-8*, *osteopontin*, *macrophage colony stimulating factor-1*, *CD44*, *proliferating peroxisome-activating receptor  $\gamma$* , and *proliferating peroxisome-activating receptor  $\delta$* . Importantly, the magnitude of gene expression progressed as the animals aged, approaching values obtained for adenomatous tissue, thus underscoring the neoplastic relevance (9). From a biochemical point of view, Moran et al. showed recently that, in the uninvolved MIN mouse mucosa, several tyrosine kinases were activated (when compared with age-matched WT mice), including the epidermal growth factor receptor and Src (22). Both epidermal growth factor receptor and Src have been shown to be increased in MIN mouse tumorigenesis along with human colorectal cancer (23). From a cellular perspective, these authors have shown that enterocyte migration, proliferation, and apoptosis were markedly altered in the histologically normal mucosa compared with WT mice (24). Furthermore, these cellular/biochemical changes were reversed by treatment with a chemopreventive agent, mirroring our findings with four-dimensional ELF (25).

Thus, there are compelling genetic and biochemical underpinnings for our findings of spectral markers alterations in the preneoplastic MIN mouse mucosa. However, for these findings to be clinically translatable, there must be evidence of a field effect in hereditary colon carcinogenesis. Fortunately, there is a wealth of biological data arguing for the field effect in familial colon cancer. For instance, in FAP (the human equivalent of the MIN mouse), there is diffuse colonic mucosal hyperproliferation with concomitant biochemical changes (e.g., increased ornithine decarboxylase; ref. 26). Similar findings with proliferation (27) have been observed in the other major autosomal dominant colorectal cancer predisposing syndrome,

hereditary nonpolyposis colorectal cancer. Additionally, markers, such as lectin immunohistochemistry, have been noted to be abnormal in the uninvolved mucosa of both FAP and hereditary nonpolyposis colorectal cancer patients (28). In patients without an inherited colorectal cancer predisposition but without a defined syndrome, proliferation in the uninvolved mucosa has been shown to correlate closely with the strength of the family history (29). Other novel molecular approaches have confirmed these cellular findings. For instance, genetic alterations, such as loss of imprinting of *insulin growth factor-II* gene, are 5.1-fold more common in subjects with a family history of colorectal neoplasia (30).

Finally, it needs to be emphasized that the robust nature of the field effect has clear applications for colorectal cancer screening in the average risk population. Clinically, the distal adenomatous polyp is a well-established biomarker of proximal neoplasia. Rectal aberrant crypt foci detected on magnifying endoscopy also correlates with neoplastic lesions in the colon (31). From a cellular perspective, apoptosis (both basal and bile salt induced; refs. 7, 8) and proliferation (32) rates in the distal colon have been shown to be associated with the presence of colonic neoplasia. Genetically, there is a dramatic up-regulation of several proto-oncogenes in the histologically normal mucosa of patients who harbor colonic neoplasia when compared with those who are neoplasia free (9). Similarly, there were marked alterations in physiologic variables, such as intracellular calcium concentrations (33) and biochemical alterations, including cytosine DNA-methyltransferase (34) and protein kinase C (13). Importantly, these cellular (6) and genetic (9) changes in the uninvolved mucosa did not seem to be markedly attenuated by distance from the neoplastic lesion. The power of the field effect is supported by the finding that expression of genes, such as *folypolyglutamate synthase*, in the uninvolved mucosa provided prognostic insights in patients with colorectal cancer (35).

To characterize the microarchitecture of the colon, we employed three previously validated spectral markers: fractal dimension, spectral slope, and PCA. Fractal dimension is a measure of the complexity and space-filling nature of a structure. This variable is well established in the fields of pathology and cancer biology (36). Indeed, it has been suggested that altered fractal dimension is one of the earliest events in colon carcinogenesis (37). Whereas fractal dimension assesses tissue organization at the cellular to the large organelle level, spectral slope is affected by much smaller structures (small organelles to macromolecular complexes). As discussed above, a greater spectral slope suggests a shift in the size distribution of intracellular structures toward smaller scales. During neoplastic transformation, we have observed a marked reduction in spectral slope, which we speculate may be secondary to aggregation of smaller intracellular structures to form large complexes. PCA is a standard data reduction technique to identify structure in a complex data set. Thus, these three spectral markers encompass a wide spectrum of tissue organization.

**Table 1. Performance characteristics of spectral markers in correctly determining the inherited susceptibility (APC status) in the mice**

	Week 6 (%)	Week 7 and 8 (%)
Positive predictive value	92	96
Negative predictive value	95	97
Sensitivity	92	96
Specificity	95	97

NOTE: Three spectral markers were assayed to classify animals. The sensitivity, specificity, positive predictive value, and negative predictive value were all >90%.

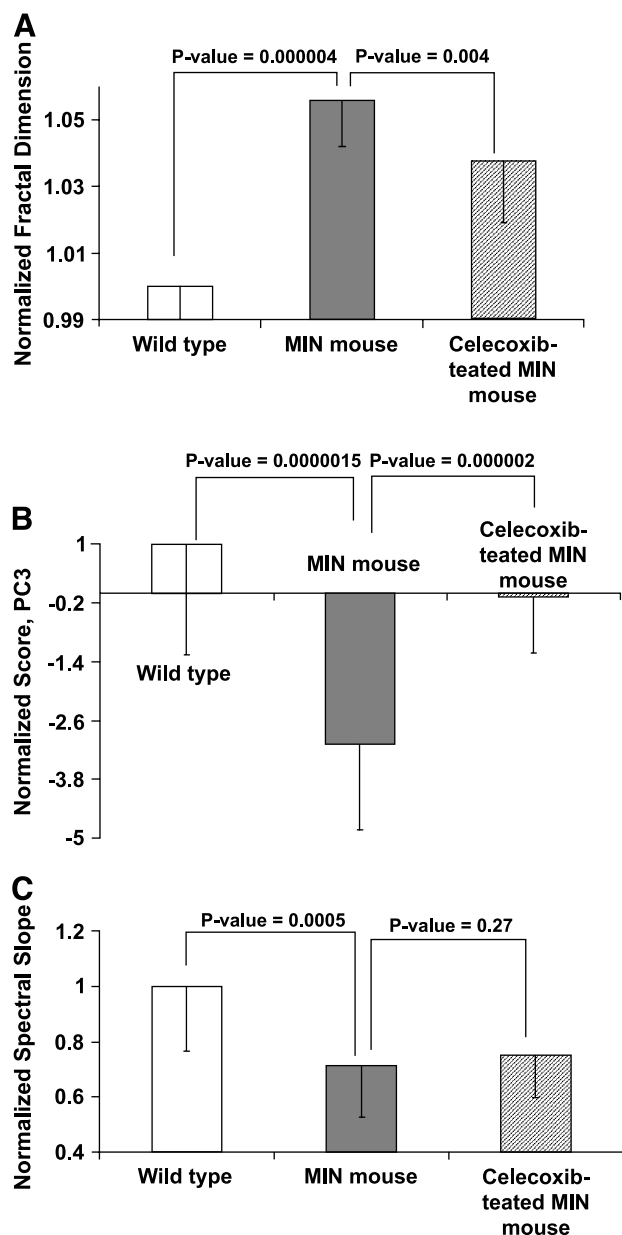


**Figure 5.** Response of spectral markers to treatment with the chemopreventive agent, celecoxib. MIN mice (7 weeks old) were treated with celecoxib 1,500 ppm for 1 week and compared with age-matched controls (both MIN and WT mice). Fractal dimension and principal component 3 were normalized (changed toward WT values) with celecoxib (A and B, respectively), whereas spectral slope was not significantly altered (C).

In the present study, we were able to accurately identify the animals that harbored germ line APC mutations before adenoma development through analysis of these spectral markers assessed in the histologically normal mucosa. We have shown previously that these markers were able to predict future aberrant crypt foci occurrence in the azoxymethane-treated rat model before aberrant crypt foci occurrence (14). The relevance to human colon carcinogenesis is supported by our preliminary data that spectral markers from colon biopsies of endoscopically normal areas had remarkable sensitivity in identifying patients who harbored adenomas (38). In the present studies with the MIN mouse, we focused our attention exclusively at the preneoplastic

stage. There was a clear spatial correlation with the occurrence of future neoplasia (small bowel  $\gg$  colon). Although we did not perform extended longitudinal studies in the MIN mouse, we did note a marked progression in the markers between the two preadenomatous time points assayed (weeks 6 and 7-8). Thus, we anticipate that, as age progresses, there would be more dramatic microarchitectural changes detected in both the small bowel and the colon. This would be consistent with the time-dependent alteration in proto-oncogene expression noted in the uninvolved intestinal mucosa in the MIN mouse (9).

An unlikely alternative explanation to our findings is that we may actually be detecting dysplastic areas. To mitigate this potential confounding factor, we exclusively focused on preneoplastic time points. As expected, we did not observe any adenomatous polyps. Using higher magnification, other groups have noted minimal tumor burden at early stages ( $6.1 \text{ mm}^2$  at week 5), which dramatically progressed over time ( $83.5 \text{ mm}^2$  at week 15; ref. 39). Thus, although possible that there may have been some contamination of our readings with adenomatous epithelium, this would be a rare event. Importantly, we obtained  $>20$  readings per animal and  $>90\%$  of the readings in the MIN mice were abnormal, making it quite improbable that the spectral marker alterations was a result of serendipitously detecting microadenomas.

To further show the relevance of these four-dimensional ELF signatures in the uninvolved mucosa to future neoplastic risk, we assessed the ability of short-term treatment with a well-established potent chemopreventive agent celecoxib. Here, we show that short-term treatment of celecoxib caused a rapid normalization of two of the three spectral markers assessed. The relevance to tumorigenesis is underscored by the demonstration that this dosage reduced MIN mouse adenomas by  $\sim 90\%$  (21). The reasons for the lack of significant modulation of spectral slope by celecoxib either may relate to the short-term (possibly some spectral markers take longer to reverse than others) or may represent the molecular mechanisms involved in chemoprevention (e.g., altered apoptosis versus proliferation). Although we did not compare the performance of spectral versus conventional markers, based on the literature, it seems that these results are markedly superior to what would be expected with classic cellular variables. Indeed, we have shown recently that a spectral marker (fractal dimension) outperformed classic conventional biomarkers (apoptosis and proliferation) in gauging antitumorigenic efficacy in the MIN mouse of antisense oligonucleotides to the transcriptional repressor SNAIL (40). Thus, we believe spectral markers may much more accurately reflect the chemopreventive efficacy than any heretofore described biomarkers.

In conclusion, we report herein, for the first time, that spectral markers are able to detect an inherited predisposition toward intestinal neoplasia at a time point that preceded phenotypic manifestation (i.e., development of intestinal adenomas). The spatial and temporal progression, along with previous validation in other models, provides compelling evidence for the relevance of these microarchitectural measures to future neoplasia. Moreover, the rapid reversal of these markers with celecoxib suggests that four-dimensional ELF assessment may represent an accurate means of gauging chemopreventive efficacy. Thus, four-dimensional ELF analysis has the potential to become a sensitive and practical means for colorectal cancer risk stratification and chemoprevention.

## References

- Jemal A, Murray T, Ward E, et al. Cancer statistics, 2005. *CA Cancer J Clin* 2005;55:10-30.
- Winawer S, Fletcher R, Rex D, et al. Colorectal cancer screening and surveillance: clinical guidelines and rationale. Update based on new evidence. *Gastroenterology* 2004;124:544-60.

3. Grady WM. Genetic testing for high-risk colon cancer patients. *Gastroenterology* 2003;124:1574-94.
4. Murff HJ, Spigel DR, Syngal S. Does this patient have a family history of cancer? An evidence-based analysis of the accuracy of family cancer history. *JAMA* 2004;292:1480-9.
5. Watson P, Ashwathnarayan R, Lynch HT, Roy HK. Tobacco use and increased colorectal cancer risk in patients with hereditary nonpolyposis colorectal cancer (Lynch syndrome). *Arch Intern Med* 2004;164:2429-31.
6. Mills SJ, Shepherd NA, Hall PA, Hastings A, Mathers JC, Gunn A. Proliferative compartment deregulation in the non-neoplastic colonic epithelium of familial adenomatous polyposis. *Gut* 1995;36:391-4.
7. Anti M, Marra G, Armelao F, et al. Rectal epithelial cell proliferation patterns as predictors of adenomatous colorectal polyp recurrence. *Gut* 1993;34:525-30.
8. Bernstein C, Bernstein H, Garewal H, et al. A bile acid-induced apoptosis assay for colon cancer risk and associated quality control studies. *Cancer Res* 1999;59:2353-7.
9. Chen LC, Hao CY, Chiu YS, et al. Alteration of gene expression in normal-appearing colon mucosa of APC<sup>min</sup> mice and human cancer patients. *Cancer Res* 2004;64:3694-700.
10. Weyn B, Jacob W, da Silva VD, et al. Data representation and reduction for chromatin texture in nuclei from premalignant prostatic, esophageal, and colonic lesions. *Cytometry* 2000;41:133-8.
11. Backman V, Wallace MB, Perelman LT, et al. Detection of preinvasive cancer cells. *Nature* 2000;406:35-6.
12. Gurjar RS, Backman V, Perelman LT, et al. Imaging human epithelial properties with polarized light-scattering spectroscopy. *Nat Med* 2001;7:1245-8.
13. Kim Y, Liu Y, Wali R, et al. Simultaneous measurement of angular, spectral, and azimuthal dependence of light scattering for characterization of tissue microarchitecture and its alteration in early precancer. *IEEE J Select Top Quant Elect* 2003;9:243-57.
14. Roy HK, Liu Y, Wali RK, et al. Four-dimensional elastic light-scattering fingerprints as preneoplastic markers in the rat model of colon carcinogenesis. *Gastroenterology* 2004;126:1071-81.
15. Wali RK, Roy HK, Kim Y, et al. Increased microvascular blood content is an early event in colon carcinogenesis. *Gut* 2005;54:654-60.
16. Wax A, Yang C, Muller M, et al. *In situ* detection of neoplastic transformation and chemopreventive effects in rat esophagus epithelium using angle-resolved low-coherence interferometry. *Cancer Res* 2003;63:3556-9.
17. Roy HK, Karolski WJ, Ratashak A. Distal bowel selectivity in the chemoprevention of experimental colon carcinogenesis by the non-steroidal anti-inflammatory drug nabumetone. *Int J Cancer* 2001;92:609-15.
18. Roy HK, Karolski WJ, Ratashak A, Smyrk TC. Chemoprevention of intestinal tumorigenesis by nabumetone: induction of apoptosis and Bcl-2 down-regulation. *Br J Cancer* 2001;84:1412-6.
19. Hoglund M, Gisselsson D, Sall T, Mitelman F. Coping with complexity. multivariate analysis of tumor karyotypes. *Cancer Genet Cytogenet* 2002;135:103-9.
20. Mori Y, Selaru FM, Sato F, et al. The impact of microsatellite instability on the molecular phenotype of colorectal tumors. *Cancer Res* 2003;63:4577-82.
21. Jacoby RF, Seibert K, Cole CE, Kelloff G, Lubet RA. The cyclooxygenase-2 inhibitor celecoxib is a potent preventive and therapeutic agent in the min mouse model of adenomatous polyposis. *Cancer Res* 2000;60:5040-4.
22. Moran AE, Hunt DH, Javid SH, Redston M, Carothers AM, Bertagnolli MM. Apc deficiency is associated with increased Egr activity in the intestinal enterocytes and adenomas of C57BL/6J-Min/+ mice. *J Biol Chem* 2004;279:43261-72.
23. Russello SV, Shore SK. SRC in human carcinogenesis. *Front Biosci* 2004;9:139-44.
24. Mahmoud NN, Bilinski RT, Churchill MR, Edelmann W, Kucherlapati R, Bertagnolli MM. Genotype-phenotype correlation in murine Apc mutation: differences in enterocyte migration and response to sulindac. *Cancer Res* 1999;59:353-9.
25. Moran AE, Carothers AM, Weyant MJ, Redston M, Bertagnolli MM. Carnosol inhibits  $\beta$ -catenin tyrosine phosphorylation and prevents adenoma formation in the C57BL/6J/Min/+ (Min/+) mouse. *Cancer Res* 2005;65:1097-104.
26. Giardiello FM, Hamilton SR, Hylind LM, Yang VW, Tamez P, Casero RA Jr. Ornithine decarboxylase and polyamines in familial adenomatous polyposis. *Cancer Res* 1997;57:199-201.
27. Lynch HT, Schuelke GS, Kimberling WJ, et al. Hereditary nonpolyposis colorectal cancer (Lynch syndromes I and II). II. Biomarker studies. *Cancer* 1985;56:939-51.
28. Sams JS, Lynch HT, Burt RW, Lanspa SJ, Boland CR. Abnormalities of lectin histochemistry in familial polyposis coli and hereditary nonpolyposis colorectal cancer. *Cancer* 1990;66:502-8.
29. Gerdes H, Gillin JS, Zimbalist E, Urmacher C, Lipkin M, Winawer SJ. Expansion of the epithelial cell proliferative compartment and frequency of adenomatous polyps in the colon correlate with the strength of family history of colorectal cancer. *Cancer Res* 1993;53:279-82.
30. Cruz-Correa M, Cui H, Giardiello FM, et al. Loss of imprinting of insulin growth factor II gene: a potential heritable biomarker for colon neoplasia predisposition. *Gastroenterology* 2004;126:964-70.
31. Takayama T, Katsuki S, Takahashi Y, et al. Aberrant crypt foci of the colon as precursors of adenoma and cancer. *N Engl J Med* 1998;339:1277-84.
32. Sahu RK, Argov S, Bernshtain E, et al. Detection of abnormal proliferation in histologically "normal" colonic biopsies using FTIR-microspectroscopy. *Scand J Gastroenterol* 2004;39:557-66.
33. Edelstein PS, Thompson SM, Davies RJ. Altered intracellular calcium regulation in human colorectal cancers and in "normal" adjacent mucosa. *Cancer Res* 1991;51:4492-4.
34. Issa JP, Vertino PM, Wu J, et al. Increased cytosine DNA-methyltransferase activity during colon cancer progression. *J Natl Cancer Inst* 1993;85:1235-40.
35. Odin E, Wettergren Y, Nilsson S, et al. Altered gene expression of folate enzymes in adjacent mucosa is associated with outcome of colorectal cancer patients. *Clin Cancer Res* 2003;9:6012-9.
36. Cross SS. Fractals in pathology. *J Pathol* 1997;182:1-8.
37. Waliszewski P, Molski M, Konarski J. On the holistic approach in cellular and cancer biology: nonlinearity, complexity, and quasi-determinism of the dynamic cellular network. *J Surg Oncol* 1998;68:70-8.
38. Horwitz J, Cohen E, Goldberg M, et al. Micro-architectural alterations in endoscopically-normal mucosa provides accurate risk stratification for colorectal neoplasia. *Am J Gastroenterol* 2004;99:A11.
39. Kettunen HL, Kettunen AS, Rautonen NE. Intestinal immune responses in wild-type and Apc<sup>min</sup>/+ mouse, a model for colon cancer. *Cancer Res* 2003;63:5136-42.
40. Roy HK, Iversen P, Hart J, et al. Down-regulation of SNAIL suppresses MIN mouse tumorigenesis: modulation of apoptosis, proliferation, and fractal dimension. *Mol Cancer Ther* 2004;3:1159-65.